Continuous-Flow Asymmetric Aldol Addition Using Immobilized Chiral Catalyst on Organogel-Based Porous Monolith

Matsumoto, Hikaru
Department of Chemical Engineering, Faculty of Engineering, Kyushu University

Hattori, Haruka
Department of Chemical Engineering, Faculty of Engineering, Kyushu University

Nagao, Masanori
Department of Chemical Engineering, Faculty of Engineering, Kyushu University

Hoshino, Yu
Department of Applied Chemistry, Faculty of Engineering, Kyushu University

他

出版情報：Journal of Chemical Engineering of Japan. 57 (1), pp.2384402-, 2024-09-13. Taylor and Francis
バージョン：

Taylor & Francis
Taylor & Francis Group

Journal of Chemical Engineering of Japan

ISSN: (Print) (Online) Journal homepage: www.tandfonline.com/journals/tjce20

Continuous-Flow Asymmetric Aldol Addition Using Immobilized Chiral Catalyst on Organogel-Based Porous Monolith

Hikaru Matsumoto, Haruka Hattori, Masanori Nagao, Yu Hoshino & Yoshiko Miura

To cite this article: Hikaru Matsumoto, Haruka Hattori, Masanori Nagao, Yu Hoshino & Yoshiko Miura (2024) Continuous-Flow Asymmetric Aldol Addition Using Immobilized Chiral Catalyst on Organogel-Based Porous Monolith, Journal of Chemical Engineering of Japan, 57:1, 2384402, DOI: 10.1080/00219592.2024.2384402

To link to this article: https://doi.org/10.1080/00219592.2024.2384402

JOURNAL OF CHEMICAL ENGINEERING OF JAPAN
2024, VOL. 57, NO. 1, 2384402
https://doi.org/10.1080/00219592.2024.2384402

Taylor & Francis
Taylor & Francis Group

RESEARCH ARTICLE

OPEN ACCESS Check for updates

Continuous-Flow Asymmetric Aldol Addition Using Immobilized Chiral Catalyst on Organogel-Based Porous Monolith

Hikaru Matsumoto[a], Haruka Hattori[a], Masanori Nagao[a], Yu Hoshino[b], and Yoshiko Miura[a]

[a]Department of Chemical Engineering, Faculty of Engineering, Kyushu University, 744 Motooka, Nishi-ku, Fukuoka, 819-0395, Japan;
[b]Department of Applied Chemistry, Faculty of Engineering, Kyushu University, 744 Motooka, Nishi-ku, Fukuoka, 819-0395, Japan

ABSTRACT

Continuous-flow reactions using immobilized chiral catalysts are attracting much attention in the field of fine chemical productions. Porous materials can mitigate the mass transfer limitation and undesired steric effects from support materials owing to their large surface area and high porosity. Among them, porous monoliths, which are self-standing materials with interconnected pores with narrow diameters offer high permeability during the continuous-flow operation. Supporting the chiral catalyst on the monolith, asymmetric reaction can be achieved under continuous-flow condition. To date, the continuous-flow reactors with porous monoliths have been developed for chiral catalysis. Herein, we first developed porous organogel monoliths as support for chiral catalyst in continuous-flow reaction. The monolith showed higher catalytic durability than those of batch in asymmetric aldol additions. Detailed studies on continuous-flow conditions and physical properties of the monolith revealed the importance of increasing the gel porosity of the monolith.

GRAPHICAL ABSTRACT

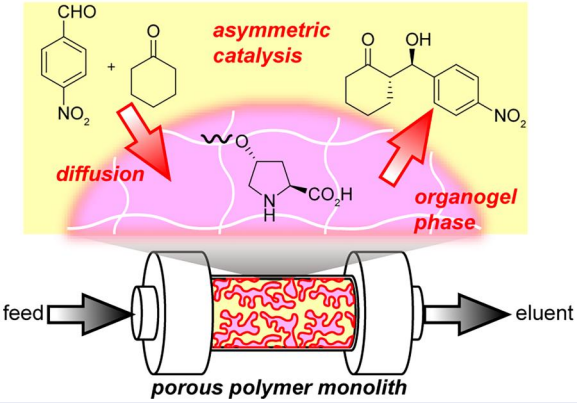

ARTICLE HISTORY
Received 21 May 2024
Accepted 21 July 2024

KEYWORDS
Porous polymer; Monolith; Continuous-flow system; Heterogeneous catalyst; Asymmetric aldol addition

1. Introduction

Continuous-flow syntheses of valuable organic compounds have become a focal point in the production of fine chemicals. Asymmetric catalysis, in particular, is important in synthesizing chiral fine chemicals, important molecules in pharmaceuticals, agrochemicals, and fragrance industries (Plutschack et al. 2017; Porta et al. 2016; Wiles and Watts 2012). Continuous-flow operations offer advantages such as sequential combinatorial syntheses, high-throughput screening, efficient heat and mass transfer, reproducibility, automation, on-demand production, and safety compared to batch systems (Britton and Raston 2017; Hartman et al. 2011). Immobilized chiral catalysts in continuous-flow reactions play a crucial role in producing these chiral fine chemicals. Typically, these catalysts are created by supporting a catalytic species on a solid material, facilitating easy recovery and reuse (Masuda et al. 2018; Kobayashi 2016; Tsubogo et al. 2013). Another important benefit of continuous-flow reactions with immobilized catalysts is the mitigation of product inhibition through automatic separation from the supported catalyst, overcoming the limitations of catalytic durability in batch processes (Tsubogo et al. 2013).

On the other hand, immobilized catalysts often exhibit relatively lower catalytic activities and selectivities compared to their homogeneous counterparts due to mass transfer

CONTACT Yoshiko Miura miuray@chem-eng.kyushu-u.ac.jp

Supplemental data for this article is available online at https://doi.org/10.1080/00219592.2024.2384402.

limitations and undesired microenvironments around the catalytic center (Goodman et al. 2017; Sun et al. 2015; Dittmeyer and Emig 2008). Porous polymers have emerged as promising solutions to address these challenges, offering large surface areas, high porosity, chemical stability, and cost-effectiveness (Debruyne et al. 2021; Liu et al. 2018). Microporous polymers, including metal-organic frameworks (MOFs) (Chen et al. 2017), covalent organic frameworks (COFs) (Ma et al. 2020; Xu et al. 2014), conjugated porous polymers (CPPs) (Zhang et al. 2012), and porous organic polymers (POPs) (Let et al. 2023), have demonstrated feasibility as chiral or achiral immobilized catalysts in continuous-flow organic transformations. However, their use in continuous-flow systems is limited due to the typical formation of these polymers as polycrystalline and/or fine powders. This leads to processing and handling difficulties within packed-bed reactors, resulting in high pressure loss, reactor clogging, stagnation zones, hot-spot formation, and a broad residence time distribution. It is necessary to shape the polymers into suitable forms, which is not an easy task (Yeskendir et al. 2021; Slater and Cooper 2015).

Fréchet and Svec first introduced porous polymer monoliths for continuous-flow applications, offering a rigid, self-supporting scaffold with high porosity and narrow pore size distribution (Svec and Frechet 1992). This design enables excellent permeability and a relatively uniform stream through the monolith column, overcoming limitations seen in packed-bed reactor systems (Chiroli et al. 2014). To further enhance immobilized catalyst performance, our research group previously developed hydrogel-based porous polymer monoliths for continuous-flow reactions (Matsumoto et al. 2017a, 2017b). The hydrogel monoliths demonstrated high permeability due to large flow-through pores and high porosity. The swollen gel network provided microporosity, facilitating the easy diffusion of small substances, promoting intimate contact with supported catalytic centers. This unique characteristic of the swollen monolith is rational and advantageous in exhibiting the inherent performance of the catalytic centers over other non-swelling porous materials in Pd-catalyzed Suzuki-Miyaura cross-couplings. While these successes in gel-based monolith reactors, the catalytic application of hydrogel was limited to aqueous solution containing dilute substrate due to the low solubility of the hydrophobic substances. The development of monolith reactors swollen with organic solvents would offer a potent catalytic system for a broad range of organic syntheses using immobilized chiral catalysts with high catalytic efficiency and hence productivity, though this concept has not been reported yet for asymmetric organic reactions.

Herein, we introduce the design and optimization of a catalytic system utilizing an organogel-based porous monolith for immobilized catalysis under continuous-flow conditions. Our model catalyst is L-proline, which is one of the well known organocatalyst and effective to asymmetric syntheses such as aldol addition, Mannich reaction, and Michael addition (Vachan et al. 2020). The proline-based vinyl monomer can be directly accessed by one step reactions between easily available starting materials (Kristensen et al. 2009). We employ a methacrylate-type polymer as the supporting material for the organogel-based monolith (Figure 1). Previously, proline-supported monolith reactors have been developed for asymmetric catalysis in a continuous-flow system. However, the turnover numbers (TONs) of the monoliths were low (up to 13), and further modulation of the material properties were required (Hattori et al. 2020; Nonaka et al. 2022). In this sense, we focused on the swelling properties of organogel-based polymer monolith. The organogel-based monolith reactor was employed in the continuous-flow aldol addition between *p*-nitrobenzaldehyde and cyclohexanone in a dimethyl sulfoxide (DMSO)/water solution. Comparative experiments with a batch system highlighted the improved catalytic durability of the monolith in the continuous-flow system (up to 36 TONs). Additionally, detailed investigations were conducted on parameters related to hydrodynamic properties and the cross-linking degree of the monoliths. The catalytic performance of the monolith reactors was correlated with the volume fraction of space where a tracer molecule could freely diffuse through the organogel, identified as a key factor in enhancing the durability of the immobilized catalyst in a continuous-flow system.

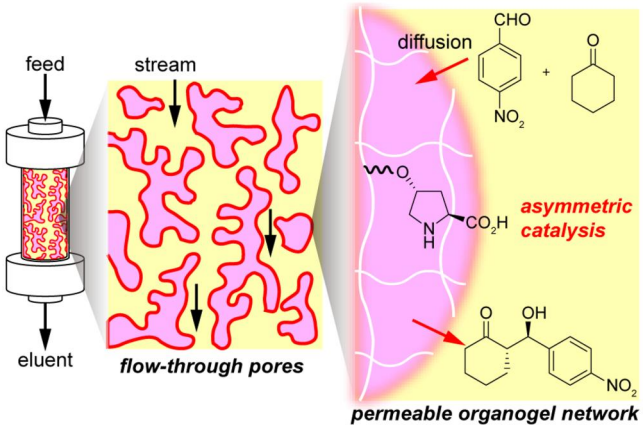

Figure 1. Schematic of organogel-based porous monolith reactor as continuous-flow immobilized catalyst.

2. Experimental

2.1. Materials

Reagents were obtained from commercial suppliers unless otherwise noted. Water with conductivity of 18.2 MΩ cm (Milli-Q, Millipore Co., Bedford, MA) was used. Butyl methacrylate (BMA, stabilized with hydroquinone, FUJIFILM Wako Pure Chemical Industry Co., Ltd., Osaka, Japan) and ethylene glycol dimethacrylate (EGDMA, stabilized with hydroquinone, Tokyo Chemical Industry Co., Ltd.) were purified using basic alumina column. *O*-methacryloyl-*trans*-4-hydroxy-L-proline hydrochloride (Pro) was synthesized according to the previous report (see supplemental data). *trans*-4-Hydroxy-L-proline (Tokyo Chemical Industry Co., Ltd., Tokyo, Japan) was dried at 70 °C for 16 h before use. 2,2'-Azobis(isobutyronitrile) (AIBN) was purified by recrystallization from MeOH.

2.2. Measurements and continuous-flow setup

Samples for field emission scanning electron microscopy (FE-SEM) analysis were coated with Pt (ca. 4 nm thickness) using an JEOL JFC-1600 auto fine coater (JEOL Ltd., Tokyo, Japan). FE-SEM analysis was performed on a Hitachi SU8000 microscopy (Hitachi High-Technologies Co., Ltd., Tokyo, Japan). Mercury intrusion porosimetry (MIP) analysis was performed on a Micromeritics AutoPoreIV9520 (Micromeritics Instrument Co., Norcross, GA, USA). SA). Fourier transform-infrared (FT-IR) spectra were recorded on a PerkinElmer Spectrum 100 FT-IR spectroscopy (PerkinElmer Inc., Waltham, MA, USA) at room temperature in air with 2 cm^{-1} spectral resolution and 100 scans. Elemental analysis (EA) was performed on a Yanako MT-6 CHN corder (Yanaco Technical Science Co., Ltd., Tokyo, Japan). Solution nuclear magnetic resonance (NMR) spectra were recorded on a JEOL ECZ400S spectroscopy, operating at 400 MHz for ^1H NMR. Chemical shifts values for ^1H NMR spectra were referenced to Me_4Si. Reverse-phase high-performance liquid chromatography (HPLC) analysis to determine yield of product was performed on a JASCO LC-2000Plus system (JASCO Co., Tokyo, Japan) equipped with a JASCO DG-980-50 degasser, a JASCO PU-980 pump, a Kanto Chemical Mightysil RP-18 GP 250-4.6 column (Kanto Chemical Co., Ltd., Tokyo, Japan), a JASCO UV-2077Plus ultraviolet (UV) detector, and a JASCO CO-2065Plus column oven, where acetonitrile/water (60:40 v/v) containing trifluoroacetic acid (TFA, 0.1 vol%) was employed as a mobile phase. Chiral HPLC analysis was performed on a JASCO LC-2000Plus system equipped with a JASCO DG-980-50 degasser, a JASCO PU-986 pump, a CHIRALPAK AD-H 250-4.6 column (Daicel Co., Ltd., Osaka, Japan), a JASCO MD-4010 photo diode array detector, and a JASCO CO-2060Plus column oven, where 2-propanol/hexane (10:90 v/v) was employed as a mobile phase. Thin-layer chromatography (TLC) analyses were performed on aluminum sheets bearing 0.17–0.22 mm layer of Merck Silica gel 60 F_{254}. Column chromatography was performed on a Biotage Isolera One flash purification system (Biotage AB Co., Uppsala, Sweden).

In continuous-flow setup, SGE glass gas-tight syringe (SGE Analytical Science Pty. Ltd., Melbourne, Australia), which was mounted on YMC YSP-101 syringe pump (YMC Co., Ltd., Kyoto, Japan), and Krone KDM-30 pressure gauge (Krone Co., Ltd., Tokyo, Japan) were connected to column in a thermo-controlled incubator with PTFE or PFA tubing (0.75 mm inner diameter). Homemade and empty columns (stainless steel, 4.0 mm inner diameter (d) × 5.0, 7.5, or 10.0 cm length (L)) were used as molds for monolith reactors.

2.3. Synthesis of porous organogel monolith catalyst

Porous monolith containing proline moiety was synthesized according to the previous reports (Figure 2a, see supplemental data) (Nonaka et al. 2022; Liu et al. 2011). Typically, EGDMA (125 mg, 0.63 mmol, $x = 37$ or 51 wt%), BMA (191 mg, 1.34 mmol, $93 - x$ wt%), and Pro (23 mg, 0.10 mmol, 7 wt%) were added to a glass vial (21.00 mm inner diameter) charged with solvent mixture of 1-PrOH/1,4-butanediol (BDO)/water (45/45/10 w/w/w, 1 mL), and the monomers were completely dissolved by shaking. AIBN (3 mg, 1 wt% with respect to the monomers) was added and completely dissolved. The monomer solution was degassed by N_2 bubbling for 30 min.

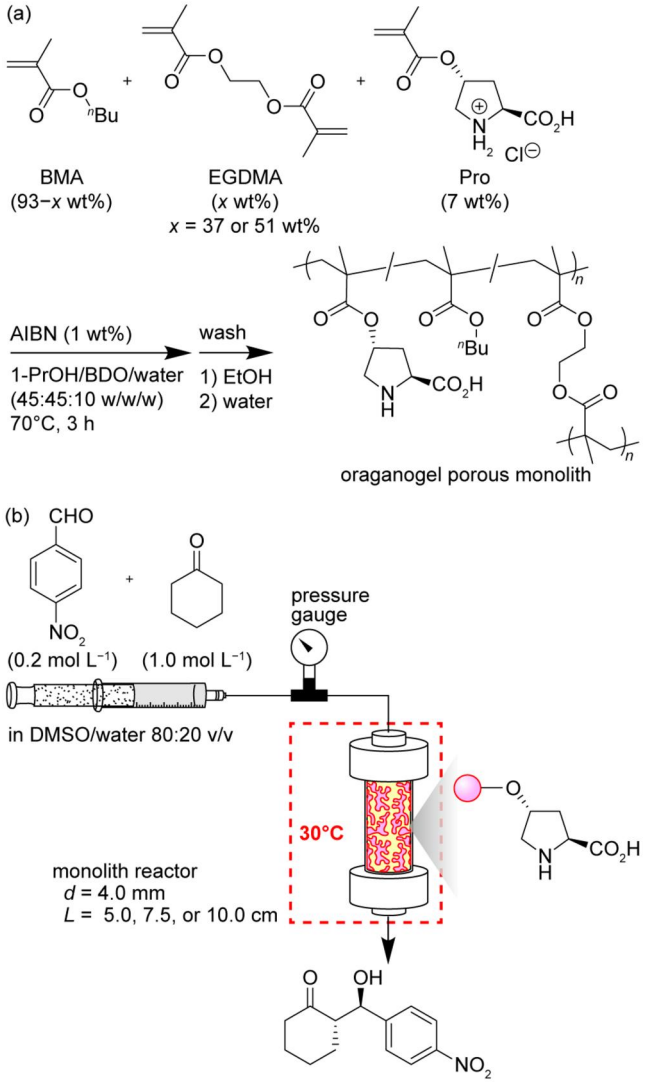

Figure 2. (a) Synthesis of proline supported organogel monoliths and (b) continuous-flow setup for asymmetric aldol addition between *p*-nitrobenzaldehyde and cyclohexanone.

For characterization, bulk monolith was prepared incubating the monomer solution in the vial at 70 °C for 3 h. Carefully crushing the vial, the resulting cylindrical polymer was washed successively by immersion in EtOH and water for 1 day each (changed more than three times per day). Complete dissociation of hydrochloric acid from the proline moiety was confirmed by neutral pH (6 ~ 7) of the water after wash. The swollen polymer was freeze-dried under vacuum to give porous monolith as white solid (305 mg, 90 wt% dry yield). Based on the results of EA for N element, the loading of proline moiety to the monolith was estimated to be 0.21–0.23 mmol g^{-1} (calculated value from feed ratio of monomers: 0.29 mmol g^{-1}).

For preparation of monolith column, stainless-steel tube (4.0 mm $d \times 5.0$, 7.5, or 10.0 cm L) was filled with the monomer solution using syringe and sealed at the ends with rubber. After incubation at 70 °C for 3 h, the seals were removed, and the column was provided with fittings and attached to a syringe pump and a pressure gauge. EtOH and water were successively permeated through the column for wash. Complete dissociation of hydrochloric acid from proline moiety was confirmed by neutral pH (6 ~ 7) of aqueous eluent. Typically, water equivalent to 20 column volume was needed for the wash. Superficial linear velocity (u) and residence time (τ) in the column were defined as follows:

$$u = \frac{Q}{\pi d^{2}/4} \tag{1}$$

$$\tau = \frac{L}{u} \tag{2}$$

where Q is flow rate of feed solution. DMSO/water mixture (80:20 v/v) was permeated through the column at various u, and the pressure loss was monitored. The Darcy's permeabilities (k_D) of columns were estimated as follows:

$$k_D = \frac{\mu L u}{\Delta P} \tag{3}$$

where μ and ΔP are viscosity of feed (LeBel and Goring 1962) and pressure loss, respectively. Based on the linear fitting of ΔP v.s. u diagram, the k_D of columns were estimated.

2.4. Catalytic tests in asymmetric aldol addition

2.4.1. Batch system

The substrates solution of *p*-nitrobenzaldehyde (30 mg, 0.20 mmol, 1 eq.) and cyclohexanone (103 mg, 1.00 mmol, 5 eq.) in DMSO/water (80:20 v/v, 1 mL) was prepared in a glass vial. Then, powdered monolith (0.02 mmol, 10 mol%) was added and mixed gently at 30 °C for 24 h. A small aliquot of the reaction mixture was taken out on a timely base, and the yield of aldol product was determined by HPLC analysis. In the case of product inhibition test, the aldol product (50 mg, 0.20 mmol, 100 mol%) was pre-mixed in a reaction solution. The reaction mixture was diluted with EtOAc and filtered through a cotton plug. The filtrate was extracted with EtOAc and washed with water. The combined organic phase was washed with brine and dried over Na_2SO_4. After filtration and evaporation, the resulting crude material was purified by flash column chromatography on silica gel (EtOAc/hexane 20:80 v/v). The diastereoselectivity and enantiomeric excess (ee) of the aldol product was determined by ^{1}H NMR and chiral HPLC analyses, respectively. The product was well-known compound with spectroscopic data in accordance with literature previously reported (Da et al. 2009).

2.4.2. Continuous-flow system

After conditioning the monolith column with DMSO/water (80:20 v/v), the substrates solution of *p*-nitrobenzaldehyde (0.2 mmol L^{-1}, 1 eq.) and cyclohexanone (1.0 mol L^{-1}, 5 eq.) in DMSO/water (80:20 v/v) was loaded into a glass syringe and attached to a syringe pump. The column was provided with fittings and attached to the syringe pump. At controlled u for desired τ, the substrates solution was continuously permeated through the column at 30 °C in a thermo-controlled incubator (Figure 2b). The elution from the column was continuously collected and analyzed using reverse-phase HPLC to determine the yield of aldol product and TON as follows:

$$\mathrm{TON} = \frac{\text{total amount of product generated}}{\text{loading of proline moiety to monolith}} \tag{4}$$

After run, DMSO/water (80:20 v/v), EtOH, and water were successively permeated through the column for wash, and the absence of the substrates and the products in the eluent was confirmed by TLC. The spent monolith was extruded from the column with stainless rod and freeze-dried under vacuum. The elution from the reactor at the time of the highest yield was extracted with EtOAc and washed with water. The combined organic phase was washed with brine and dried over Na_2SO_4. After filtration and evaporation, the resulting crude material was purified by flash column chromatography on silica gel (EtOAc/hexane 20:80 v/v). The diastereoselectivity and ee of the aldol product was determined by ^{1}H NMR and chiral HPLC analyses, respectively.

2.5. Evaluation of gel porosity of organogel monolith column

Proline-free organogel monoliths were prepared in home-made and empty columns (stainless steel, 4.0 mm $d \times 5.0$, 7.5, or 10.0 cm L) by copolymerization of BMA (100−x wt%) and EGDMA ($x = 37$ or 51 wt%) in the absence of Pro. The resulting column was washed withing with EtOH and water, and conditioning with DMSO/water (80:20 v/v). *p*-Nitrobenzaldehyde (0.2 mol L^{-1}) was dissolved as a tracer in DMSO/water (80:20 v/v), and the solution was loaded into a glass syringe on a syringe pump. The column was provided with fittings and attached to the syringe. At controlled Q for desired τ, the tracer solution was continuously permeated through the column (step input). The elution from the column was continuously collected and analyzed using reverse-phase HPLC to determine the concentration of tracer to obtain the breakthrough curves of tracer ($C(t)/C_0$ v.s. t diagrams). A gel porosity (ε_g), meaning the sum of the volume of flow-through pores and micropores within the gel phase in the monolith was defined as follows (Nischang 2012; Jerabek 1985):

$$\varepsilon_g = 1 - \frac{V_{\mathrm{dead}} + V_{\mathrm{monolith}} - \int Q\left(1 - \frac{C(t)}{C_0}\right)dt}{V_{\mathrm{monolith}}} \times 100 \tag{5}$$

Where t, $C(t)$, C_0, V_{dead}, and V_{monolith} represent time, concentration of tracer in the eluent at $t = t$, concentration of tracer in the feed, dead volume including tubings from the syringe to a sampling position, and geometrical swelling

volume of monolith (calculated by inner diameter and length of the column), respectively.

3. Results and Discussion

3.1. Characterization of porous monolith

Organogel-based porous monolith was synthesized via the radical copolymerization of methacrylate-type monomers. In the previous work, we utilized poly(ethylene glycol) (PEG) as a porogen to create the porous structure of the monolith (Nonaka et al. 2022). However, the high viscosity of PEG led to elevated pressures during permeation for washing, resulting in problematic clogging of the monolith column. Given this consideration, we opted for a solvent mixture of 1-PrOH/BDO/water as the porogen (Liu et al. 2011) because of its low viscosity. Monomer solution containing BMA ($93-x$ wt%), EGDMA ($x=37$ or 51 wt%), Pro (7 wt%), and AIBN (1 wt% with respect to total monomer) was prepared in the solvent mixture of 1-PrOH/BDO/water (45:45:10 w/w/w). After incubating the monomer solution at 70 °C for 3 h, the resulting self-standing polymer was successively washed with EtOH and water, and dried under vacuum to afford polymer monolith with high yield (90 wt% dry yield, $x=37$%) (Figure 2a). The field emission-scanning electron microscopy (FE-SEM) observations of the dried monoliths revealed the presence of interstitial pores between microglobules (Figures 3a and S1, see supplemental data). By MIP analyses, narrow pore size distributions of the monoliths were measured, and median pore diameters were 2700 and 3520 nm for $x=37$ and 51 wt%, respectively (Figures 3b and S2, and Table S1). Successfully, the monoliths exhibited large flow-through pores with narrow diameter distributions, contributing to a continuous-flow system characterized by high permeability and efficient mass transfer.

To prepare an organogel monolith reactor, the monomer solution was polymerized in a stainless-steel tube (4.0 mm $d\times$ 5.0, 7.5, or 10.0 cm L). The column with fittings was washed subsequently with solvent in a continuous-flow system to afford a monolith reactor. DMSO/water mixture (80:20 v/v) was continuously permeated through the column reactor at various u, and the ΔP was monitored. The ΔP was measured in duplicate in two independent experiments. The k_D of the monolith columns ($L=5.0$, 7.5, or 10.0 cm) ranged 1.4–3.1 $\times 10^{-13}$ m^2 (Figure 3c). These k_D values were notably higher than those of packed-bed column of silica particles ($k=1.1$–3.5×10^{-14} m^2 for 3–5 mm particle diameters) used in HPLC system (Jung et al. 2009). Hence, the excellent permeabilities of the porous monolith columns were highlighted featuring the large flow-through pores and high porosities. Using this proline catalyst on the organogel-based monolith, continuous-flow reactions would be smoothly realized.

3.2. Catalytic durability in batch system

The catalytic performance of the monolith was preliminarily assessed in a batch system (Table 1). The aldol addition

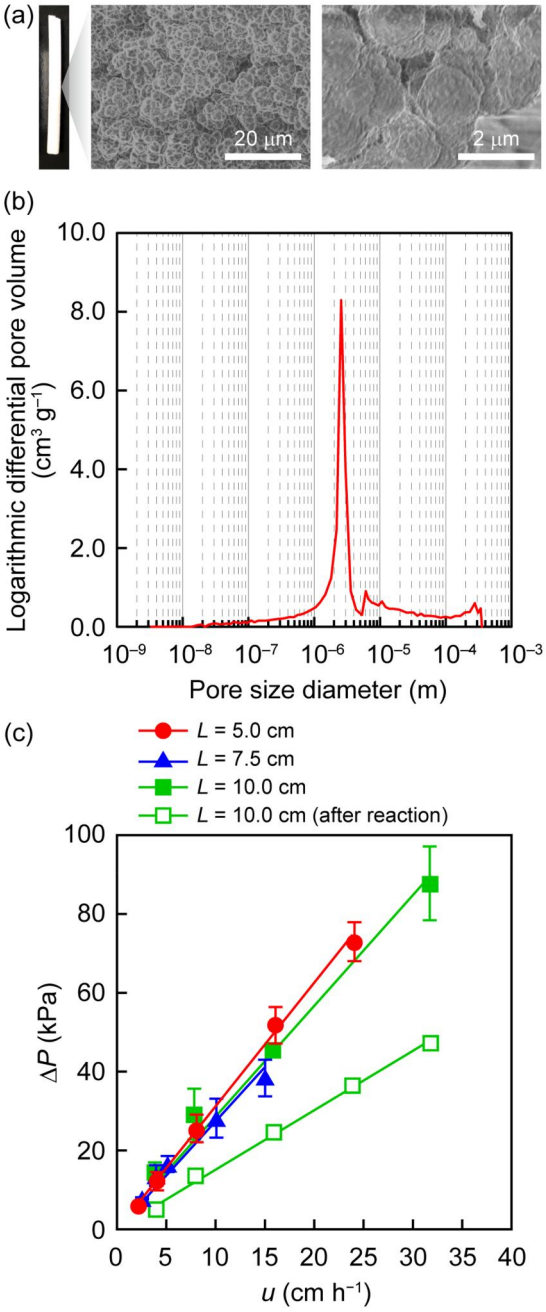

Figure 3. (a) Photographic (left) and FE-SEM images (center and right), (b) pore size distribution determined by MIP, and (c) continuous-flow permeability of the monolith ($x=37$ wt%, measured in duplicate in two independent experiments for monoliths before flow reactions).

between *p*-nitrobenzaldehyde (0.20 mol L^{-1}, 1 eq.) and cyclohexanone (1.0 mol L^{-1}, 5 eq.) was conducted using dried monolith, and the reaction mixture was analyzed using HPLC. It has been reported that the presence of water had great influence on catalytic activity and durability of L-proline catalysts in the aldol addition reactions (Zotova et al. 2007; Nakashima and Yamamoto 2018). In the present study, DMSO/water mixture was used to obtain homogeneous reaction mixture, which can be applied to continuous-flow reactions. With catalyst loading of 10.0 mol%, the TON reached 8 (entry 1, Table 1). Further reduction in catalyst loading (3.3 mol%) gave the TON of 16, which then plateaued (entries 2 and 3, Table 1). It is noteworthy that,

Table 1. Asymmetric aldol additions in batch.[a].

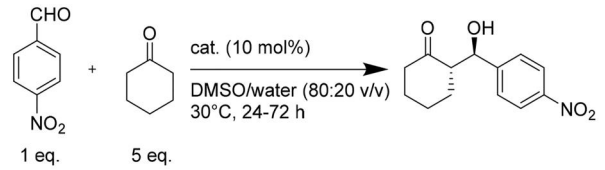

Entry	Cat. (mol%)	Time (h)	TON (-)[b]	*anti*/syn[c]	ee (%)[d]
1	10.0	24	8	90:10	96
2	3.3	48	16	n.d.	n.d.
3	3.3	72	16	90:10	96
4[e]	10.0	24	6	n.d.	n.d.
5[e]	3.3	72	9	n.d.	n.d.

[a] Conditions: p-nitrobenzaldehyde (0.20 mmol, 1 eq.), cyclohexanone (1.00 mmol, 5 eq.), monolith catalyst (x = 37 wt%), DMSO/water (80:20 v/v, 1 mL), 30 °C. b Determined by reverse-phase HPLC. c Determined by 1H NMR. d Determined by chiral HPLC. e Aldol product (100 mol%) was dosed before addition of catalyst.

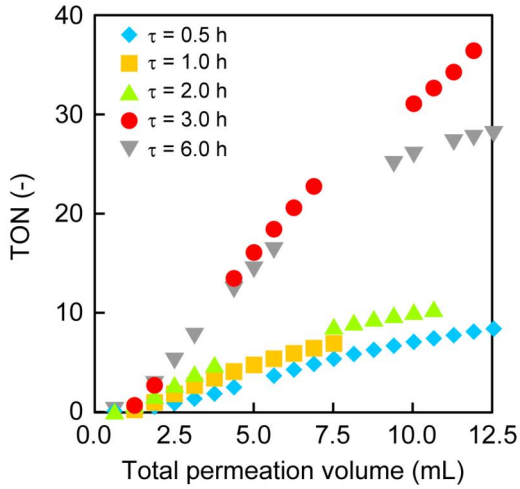

Figure 4. TONs of proline-supported monolith reactors at different residence time (τ) in continuous-flow asymmetric aldol additions. Conditions: *p*-nitrobenzaldehyde (0.2 mol L^{-1}, 1 eq.) and cyclohexanone (1.0 mol L^{-1}, 5 eq.) in DMSO/water (80:20 v/v), organogel monolith column ($x = 37$ wt%, $L = 5.0$ cm), and 30 °C.

dosing the excess of aldol product (100 mol%) before adding the catalyst (10 and 3.3 mol%) to the reaction mixture resulted in decreased the TON (6 and 9, entry 4 and 5, Table 1).

The observed phenomenon clearly indicated a severe product inhibition. It was anticipated that the gradual accumulation of aldol product poisoned supported proline in the batch system, as previously reported in the system involving proline derivatives (Mager and Zeitler 2010). On the contrary, it was anticipated that the continuous-flow system would enhance catalytic activity by facilitating the automatic separation of the aldol product, thereby mitigating the issue of product inhibition (Tsubogo et al. 2013).

3.3. Catalytic durability in continuous-flow system

3.3.1. Effect of residence time

The organogel monolith reactors were assessed in aldol addition under continuous-flow conditions (Figure 2b).

Table 2. Effect of linear velocity (*u*) and cross-linking degree (*x*) on asymmetric aldol additions with proline-supported monolith reactors[a].

Entry	*x* (wt%)	*L* (cm)	*u* (cm h^{-1})	TON (-)[b,c]	*anti*/syn[d]	ee (%)[e]
1	37	5.0	1.7	36	91: 9	96
2	37	7.5	2.5	7	91: 9	96
3	37	10.0	3.3	12	90:10	96
4	51	5.0	1.7	13	87:13	92

[a] Conditions: *p*-nitrobenzaldehyde (0.2 mol L^{-1}, 1 eq.) and cyclohexanone (1.0 mol L^{-1}, 5 eq.) in DMSO/water (80:20 v/v), organogel monolith column, $\tau = 3.0$ h, and 30 °C. [b] Determined by reverse-phase HPLC. [c] Estimated within total permeation volume = 12.5 mL. [d] Determined by ^{1}H NMR. [e] Determined by chiral HPLC.

p-Nitrobenzaldehyde (0.20 mol L^{-1}, 1 eq.) and cyclohexanone (1.0 mol L^{-1}, 5 eq.) in DMSO/water (80:20 v/v) were permeated through the monolith reactor ($L = 5.0$ cm) at various τ by varying the *u* of the substrates solution. Eluent from the reactor was continuously collected and analyzed using HPLC. Increasing the τ from 0.5 to 3.0 h, the proline-supported monolith significantly improved TONs (from 7 to 36) (Figure 4). Further elongation of the τ (6.0 h) decreased TON (28). The diastereoselectivity and ee of the aldol product at $\tau = 3$ h were measured by HPLC analyses, affording as high as *anti*/*syn* = 91:9 and 96%, respectively (entry 1, Table 2). In the continuous-flow condition, the selectivities of organogel monolith were comparable with those in batch conditions (Table 1).

Increasing τ allowed sufficient reaction time for the substrates on the monolith, resulting in high TONs (Figure 4). However, excessively long retention of the reaction solution led to a deterioration in TONs, presumably due to backmixing of the stream (Hartman et al. 2011). Minimal differences of morphologies (Figure S1, see supplemental data) and porous properties (Figure S2 and Table S1) were observed for the fresh and spent monoliths. On the other hand, the permeability of the spent column increased (Figure 3c), which indicated the changes in fluid dynamics through the spent monoliths. As the liquid permeability could be affected by the swelling properties of the monoliths in the column (Li et al. 2011), the spent monolith might show different swelling behavior against reactions mixture. It was suggested that the aldol product formed adducts with supported proline, as confirmed by FT-IR analyses of the spent monolith (Figure S3, see supplemental data). The accumulation of the aldol product within the monolith column might cause the swelling properties changing and deactivation of the catalytic cycle of proline. It has been reported that the deactivation via decarboxylation of L-proline moiety on silica-supported catalyst during continuous-flow aldol addition (Massi et al. 2011). However, the carbonyl bands (1634 cm^{-1}) of proline moiety and aldol product were overlapped. In this case, we could not deny the possibility of decarboxylation of proline during the catalytic reactions. Though the decarboxylation might cause the deactivation of proline on the monolith, the TON drastically improved by flow operation. In this sense, we attributed the main deactivation pathway to the product inhibition, which was effectively suppressed by continuous-flow operation. After all, the best TON (36) of the monolith was achieved in the continuous-flow system at $\tau = 3.0$ h (Figure 4), which

were 2.7 and 3.3-times higher than those in the batch (16 TON, entry 3, Table 1) and previously reported monolith column (13 TON) (Nonaka et al. 2022). The organogel monolith reactor demonstrated excellent catalytic durability, characterized by the automatic separation of the aldol product to minimize the potential for product inhibition of supported proline.

Furthermore, we performed the recycling test of organogel monolith in continuous-flow aldol addition (see supplemental data). After 1st run in the aldol addition, the spent monolith column was washed with DMSO/water and EtOAc, which was subsequently reused in 2nd run. This provided the comparable catalytic activity with that of the monolith used in a single run (Figure S6). Successfully, the monolith column possessed high recyclability and catalytic durability in the aldol addition under continuous-flow condition.

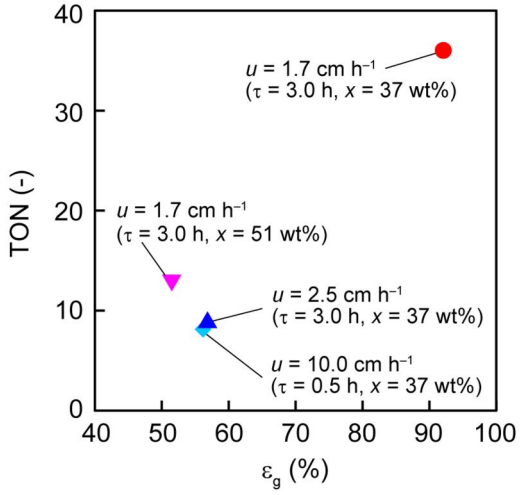

Figure 5. Relationship between TON and gel porosity (ε_g) of organogel monolith reactor in continuous-flow asymmetric aldol additions.

3.3.2. Effect of linear velocity and cross-linking degree

Having confirmed the importance of continuous-flow operation and tuning τ for achieving high TON, we next investigated the importance of u, which was defined as the distance moved by the solution per unit time relative to the direction of movement. The u is directly related to Reynolds number (Re), an index of the degree of mixing and turbulence in a continuous-flow reactor. Increasing u results in a higher Re, providing efficient mixing for enhanced catalytic activities (Klaewkla et al. 2011). In this experiment, it is crucial to adjust the L proportionally to u changes to maintain a constant reaction time in flow (τ = 3 h). For this purpose, the monolith columns were prepared by adjusting L from 5.0 to 10.0 cm and applied to continuous-flow catalysis. The u of the substrate solution ranged from 1.7 to 3.3 cm h^{-1} for each monolith reactor in accordance with the increasing L of the monolith columns. Interestingly, contrary to expectations, increasing u from 1.7 to 2.5 cm h^{-1} significantly decreased TONs (from 36 to 7) (entries 1 and 2, Table 2, and Figure S4, see supplemental data). Further increase in u had a positive effect on the TONs (from 7 to 12) (entries 2 and 3, Table 2, and Figure S4). On the other hand, u did not influence selectivities (90:10–91:9 *anti*/*syn* and 96% ee, entries 1–3, Table 2).

It has been reported that higher u leads to increased catalytic activities in porous silica monolith reactors for esterification and Diels–Alder reactions (Koreniuk et al. 2015; Sachse et al. 2012). In our system, the similar behavior of TON (from 7 to 12) was observed in the range of u from 2.5 to 3.3 cm h^{-1} (entries 2 and 3, Table 2). In contrast, the higher TONs were achieved in the slower u regions (1.7 to 2.5 cm h^{-1}) (entries 1 and 2, Table 2). The unique trend in catalytic durability might be attributed to the swollen features of the organogel monoliths. For comparative experiments, we assessed the higher cross-linking degree (x = 51 wt%) of the monolith reactor to investigate the catalytic durability of a less swollen organogel at fixed τ and u. (3.0 h and 1.7 cm h^{-1}) (entry 4, Table 2, and Figure S4, see supplemental data). As a result, a poor TON (13) was observed along with slightly lower selectivities (87:13 *anti*/*syn* and 92% ee). Increasing the x of the organogel monolith caused steric hindrance around the supported proline, resulting in an unfavorable microenvironment for the diffusion of reactants (Matsumoto et al. 2017a).

3.4. Gel porosity of organogel monolith

We further evaluated the swelling volume fraction of the gel phase, where substances could diffuse, within the organogel monolith column. In a continuous-flow system with proline-free monolith column, a solution of *p*-nitrobenzaldehyde in DMSO/water (80:20 v/v) was injected as a tracer in a step input manner, and the concentration change of elution was monitored (Figure S5, see supplemental data). The volume fraction of the feed solution required to replace all the gel phase in the monolith, i.e., gel porosity (ε_g), was estimated (Figure 5). It was surprising that decreasing both u and x drastically increased the ε_g of the monolith (up to 92%). Additionally, the larger ε_g corresponded to higher TON (Figure 5). As the ε_g reflects the accessibility of reactants toward the catalyst, large ε_g indicated the smooth transport of reactants to supported catalyst, leading to high TON of the immobilized catalyst. Hence, the remarkably high diffusivity in the organogel monolith provided almost the full space of the reactor for efficient and durable immobilized catalysis.

4. Conclusion

We have developed a porous polymer monolith with high permeability and intra-diffusivity as a catalytic reaction platform under continuous-flow conditions. The porous organogel monolith containing L-proline was fabricated as a column reactor and applied to the asymmetric aldol addition between *p*-nitrobenzaldehyde and cyclohexanone in DMSO/water under continuous-flow conditions. The catalytic performance of the monolith was considerably higher under continuous-flow conditions than under batch conditions, indicating effective suppression of product inhibition in a

continuous-flow catalytic reactor. Furthermore, tuning residence time as well as the linear velocity of the feed and cross-linking degree was important for improving catalytic activity and selectivity, which correlated with the extent of product inhibition and gel porosity within the monolith reactor. The organogel-based immobilized catalyst provided a unique microenvironment for remarkably high diffusivity and an ideal chiral center, advantageous for asymmetric catalytic reactions under continuous-flow conditions. The unique characteristics of the swollen monolith catalyst are rational and versatile for preparing and functionalizing immobilized catalysts for highly efficient continuous-flow reactions. The conceptual design of the organogel network should further expand the scope of organic transformations with high catalytic performance.

Author Contributions

H. Hattori, H. Matsumoto, and Y. Miura designed the experiments. H. Hattori performed the experiments. H. Hattori and H. Matsumoto wrote the manuscript. M. Nagao and Y. Hoshino made contributions to the discussions during the work. All authors have given approval to the final version of the manuscript.

Disclosure Statement

No potential conflict of interest was reported by the author(s).

Funding

This work was supported by JSPS KAKENHI grant numbers JP24K17560, JP 23K26708, JP23H02015, JP22H04553, JP22H05372, and JP22K19068, the Sumitomo Foundation, and the Yashima Environment Technology Foundation.

ORCID

Hikaru Matsumoto http://orcid.org/0009-0004-8004-9521
Masanori Nagao http://orcid.org/0000-0002-8387-7259
Yu Hoshino http://orcid.org/0000-0001-9628-6979
Yoshiko Miura http://orcid.org/0000-0001-8590-6079

References

Britton J, Raston CL. 2017. Multi-step continuous-flow synthesis. Chem Soc Rev. 46:1250–1271. doi: 10.1039/C6CS00830E.

Chen X, Jiang H, Hou B, Gong W, Liu Y, Cui Y. 2017. Boosting chemical stability, catalytic activity, and enantioselectivity of metal–organic frameworks for batch and flow reactions. J Am Chem Soc. 139:13476–13482. doi: 10.1021/jacs.7b06459.

Chiroli V, Benaglia M, Puglisi A, Porta R, Jumde RP, Mandoli A. 2014. A chiral organocatalytic polymer-based monolithic reactor. Green Chem. 16:2798–2806. doi: 10.1039/c4gc00031e.

Da CS, Che LP, Guo QP, Wu FC, Ma X, Jia YNJ. 2009. 2,4-dinitrophenol as an effective cocatalyst: Greatly improving the activities and enantioselectivities of primary amine organocatalysts for asymmetric aldol reactions. J Org Chem. 74:2541–2546. doi: 10.1021/jo802758b.

Debruyne M, Speybroeck V, Van Voort P, Van-Der, Stevens CV. 2021. Porous organic polymers as metal free heterogeneous organocatalysts. Green Chem. 23:7361–7434. doi: 10.1039/D1GC02319E.

Dittmeyer R, Emig G. 2008. Kinetics and transport processes. In: Ertl G, Knözinger H, Schüth F, Weitkamp J, editors. Handbook of heterogeneous catalysis. Vol. 1. 1st ed. Weinheim (Germany): WileyVCH. p. 1727–1784.

Goodman ED, Schwalbe JA, Cargnello M. 2017. Mechanistic understanding and the rational design of sinter-resistant heterogeneous catalysts. ACS Catal. 7:7156–7173. doi: 10.1021/acscatal.7b01975.

Hartman RL, McMullen JP, Jensen KF. 2011. Deciding whether to go with the flow: evaluating the merits of flow reactors for synthesis. Angew Chem Int Ed Engl. 50:7502–7519. doi: 10.1002/anie.201004637.

Hattori H, Matsumoto H, Hoshino Y, Miura Y. 2020. Development of macroporous polymer monolith immobilizing L-proline-based organocatalyst and application to flow asymmetric aldol addition reaction. Kagaku Kogaku Ronbun. 46:77–83. doi: 10.1252/kakoronbunshu.46.77.

Jerabek K. 1985. Characterization of swollen polymer gels using size exclusion chromatography. Anal Chem. 57:1598–1602. doi: 10.1021/ac00285a023.

Jung S, Ehlert S, Mora JA, Kraiczek K, Dittmann M, Rozing GP, Tallarek U. 2009. Packing density, permeability, and separation efficiency of packed microchips at different particle-aspect ratios. J Chromatogr A. 1216:264–273. doi: 10.1016/j.chroma.2008.11.073.

Klaewkla R, Arend M, Hoelderich WF. 2011. A review of mass transfer controlling the reaction rate in heterogeneous catalytic systems. In: Nakajima H, editor. Mass transfer-advanced aspects. Vol. 1. 1st ed. London (UK): IntechOpen. p. 667–684.

Kobayashi S. 2016. Flow "fine" synthesis: high yielding and selective organic synthesis by flow methods. Chem Asian J. 11:425–436. doi: 10.1002/asia.201500916.

Koreniuk A, Maresz K, Odrozek K, Jarzębski AB, Mrowiec-Białoń J. 2015. Highly effective continuous-flow monolithic silica microreactors for acid catalyzed processes. Appl Catal A. 489:203–208. doi: 10.1016/j.apcata.2014.10.047.

Kristensen TE, Vestli K, Fredriksen KA, Hansen FK, Hansen T. 2009. Synthesis of acrylic polymer beads for solid-supported proline-derived organocatalysts. Org Lett. 11:2968–2971. doi: 10.1021/ol901134v.

LeBel RG, Goring DAI. 1962. Density, viscosity, refractive index, and hygroscopicity of mixtures of water and dimethyl sulfoxide. J Chem Eng Data. 7:100–101. doi: 10.1021/je60012a032.

Let S, Dam GK, Fajal S, Ghosh SK. 2023. Organic porous heterogeneous composite with antagonistic catalytic sites as a cascade catalyst for continuous flow reaction. Chem Sci. 14:10591–10601. doi: 10.1039/D3SC03525E.

Li Y, Tolley HD, Lee ML. 2011. Preparation of monoliths from single crosslinking monomers for reversed-phase capillary chromatography of small molecules. J Chromatogr A. 1218:1399–1408. doi: 10.1016/j.chroma.2011.01.028.

Liu L, Cheng J, Matsadiq G, Li JK. 2011. Novel polymer monolith microextraction using a poly-(methyl methacrylate-co-ethylene dimethacrylate) monolith and its application to the determination of polychlorinated biphenyls in water samples. Chemosphere. 83:1307–1312. doi: 10.1016/j.chemosphere.2011.04.020.

Liu X, Tang B, Long J, Zhang W, Liu X, Mirza Z. 2018. The development of MOFs-based nanomaterials in heterogeneous organocatalysis. Sci Bull (Beijing). 63:502–524. doi: 10.1016/j.scib.2018.03.009.

Ma HC, Chen GJ, Huang F, Dong YB. 2020. Homochiral covalent organic framework for catalytic asymmetric synthesis of a drug intermediate. J Am Chem Soc. 142:12574–12578. doi: 10.1021/jacs.0c04722.

Mager T, Zeitler K. 2010. Efficient, enantioselective iminium catalysis with an immobilized, recyclable diarylprolinol silyl ether catalyst. Org Lett. 12:1480–1483. doi: 10.1021/ol100166z.

Massi A, Cavazzini AD, Zoppo L, Pandoli O, Costa V, Pasti L, Giovannini PP. 2011. Toward the optimization of continuous-flow aldol and α-amination reactions by means of proline-functionalized silicon packed-bed microreactors. Tetrahedron Lett. 52:619–622. doi: 10.1016/j.tetlet.2010.11.157.

Masuda K, Ichitsuka T, Koumura N, Sato K, Kobayashi S. 2018. Flow fine synthesis with heterogeneous catalysts. Tetrahedron. 74:1705–1730. doi: 10.1016/j.tet.2018.02.006.

Matsumoto H, Seto H, Akiyoshi T, Shibuya M, Hoshino Y, Miura Y. 2017. Macroporous gel with a permeable reaction platform for catalytic flow synthesis. ACS Omega. 2:8796–8802. doi: 10.1021/acsomega.7b00909.

Matsumoto H, Seto H, Akiyoshi T, Shibuya M, Hoshino Y, Miura Y. 2017. Macroporous monolith with polymer gel matrix as continuous-flow catalytic reactor. Chem Lett. 46:1065–1067. doi: 10.1246/cl.170360.

Nakashima H, Yamamoto E. 2018. Process catalyst mass efficiency by using proline tetrazole column-flow system. Chemistry. 24:1076–1079. doi: 10.1002/chem.201705982.

Nischang I. 2012. On the chromatographic efficiency of analytical scale column format porous polymer monoliths: Interplay of morphology and nanoscale gel porosity. J Chromatogr A. 1236:152–163. doi: 10.1016/j.chroma.2012.03.017.

Nonaka S, Matsumoto H, Nagao M, Hoshino Y, Miura Y. 2022. Investigation of the effect of microflow reactor diameter on condensation reactions in L-proline-immobilized polymer monoliths. React Chem Eng. 7:55–60. doi: 10.1039/D1RE00386K.

Plutschack MB, Pieber B, Gilmore K, Seeberger PH. 2017. The Hitchhiker's guide to flow chemistry ||. Chem Rev. 117:11796–11893. doi: 10.1021/acs.chemrev.7b00183.

Porta R, Benaglia M, Puglisi A. 2016. Flow chemistry: recent developments in the synthesis of pharmaceutical products. Org Process Res Dev. 20:2–25. doi: 10.1021/acs.oprd.5b00325.

Sachse A, Hulea V, Finiels A, Coq B, Fajula F, Galarneau A. 2012. Alumina-grafted macro-/mesoporous silica monoliths as continuous flow microreactors for the Diels–Alder reaction. J Catal. 287:62–67. doi: 10.1016/j.jcat.2011.12.003.

Slater AG, Cooper AI. 2015. Function-led design of new porous materials. Science. 348:aaa8075. doi: 10.1126/science.aaa807.

Sun Q, Dai Z, Meng X, Wang L, Xiao FS. 2015. Task-specific design of porous polymer heterogeneous catalysts beyond homogeneous counterparts. ACS Catal. 5:4556–4567. doi: 10.1021/acscatal.5b00757.

Svec F, Frechet JMJ. 1992. Continuous rods of macroporous polymer as high-performance liquid chromatography separation media. Anal Chem. 64:820–822. doi: 10.1021/ac00031a022.

Tsubogo T, Ishiwata T, Kobayashi S. 2013. Asymmetric carbon–carbon bond formation under continuous-flow conditions with chiral heterogeneous catalysts. Angew Chem Int Ed Engl. 52:6590–6604. doi: 10.1002/anie.201210066.

Vachan BS, Karuppasamy M, Vinoth P, Vivek Kumar S, Perumal S, Sridharan V, Menéndez JC. 2020. Proline and its derivatives as organocatalysts for multi-component reactions in aqueous media: synergic pathways to the green synthesis of heterocycles. Adv Synth Catal. 362:87–110. doi: 10.1002/adsc.201900558.

Wiles C, Watts P. 2012. Continuous flow reactors: a perspective. Green Chem. 14:38–54. doi: 10.1039/C1GC16022B.

Xu H, Chen X, Gao J, Lin J, Addicoat M, Irle S, Jiang D. 2014. Catalytic covalent organic frameworks via pore surface engineering. Chem Commun (Camb). 50:1292–1294. doi: 10.1039/C3CC48813F.

Yeskendir B, Dacquin JP, Lorgouilloux Y, Courtois C, Royer S, Dhainaut J. 2021. From metal–organic framework powders to shaped solids: recent developments and challenges. Mater Adv. 2:7139–7186. doi: 10.1039/D1MA00630D.

Zhang Y, Zhang Y, Sun YL, Du X, Shi JY, Wang WD, Wang W. 2012. 4-(*N*,*N*-Dimethylamino)pyridine-embedded nanoporous conjugated polymer as a highly active heterogeneous organocatalyst. Chemistry. 18:6328–6334. doi: 10.1002/chem.201103028.

Zotova N, Franzke A, Armstrong A, Blackmond DG. 2007. Clarification of the role of water in proline-mediated aldol reactions. J Am Chem Soc. 129:15100–15101. doi: 10.1021/ja0738881.